Channel Tracking for a Multi-Antenna ITS System Based on Vehicle-to-Vehicle Tunnel Measurements

Georg Maier*, Alexander Paier†, and Christoph F. Mecklenbräuker*
*Institute of Telecommunications, Vienna University of Technology
Gusshausstrasse 25/389, 1040 Vienna, Austria
Telephone: +43 1 58801-38976 Fax: +43 1 58801-38999
†Kapsch TrafficCom AG, Vienna, Austria
Email: gmaier@nt.tuwien.ac.at

***Abstract*—Traffic safety is one of the key applications for Intelligent Transport Systems (ITS). In order to meet the strict requirements of safety related wireless communication a robust and reliable radio link is necessary. The complex vehicular environment, from a radio propagation viewpoint, represents a challenge for the receiver. We show that even under poor receive conditions the use of multiple antennas and a low-complexity channel tracking algorithm improves the receiver performance. The analysis is performed on data obtained from real-world vehicle-to-vehicle (V2V) tunnel measurements in line-of-sight (LOS), non line-of-sight (NLOS), and overtaking scenarios. In this contribution we apply and extend the pilot-assisted channel tracking (PACT) algorithm to a multi antenna receiver for IEEE 802.11p. The achievable improvement of the frame success ratio (FSR) of a two antenna receiver compared to a single antenna receiver is up to 26 % (without any channel tracking). Using pilot-assisted channel tracking the FSR is further increased by 12 %.**

***Index Terms*—Vehicular communications, WAVE, ITS-G5, vehicle-to-vehicle, IEEE 802.11p, receive diversity, channel tracking, measurements.**

I. Introduction

Recently, intelligent transport systems (ITS) attracted interest in industry and academic research [1]. They offer the potential to increase the traffic safety, enhance the traffic efficiency, and improve the driving comfort. Future vehicles will receive information about their surrounding via vehicle-to-infrastructure (V2I) and vehicle-to-vehicle, collectively referred to as vehicle-to-X (V2X), communication systems.

The decision of the European commission, in August 2008, to use the 5857-5905 MHz frequency band exclusively for safety-related ITS applications also highlights the importance of ITS. ITS-G5 [2] (the European standard) and WAVE (the North American standard) are based on the physical layer (PHY) on the IEEE 802.11p standard [3]. This standard is an approved amendment of the Wireless Local Area Network (WLAN) IEEE 802.11a standard [4]. Since the IEEE 802.11a standard was designed for low user mobility, it shows weaker performance under vehicular channel conditions. One of the main differences compared to IEEE 802.11a is the doubling of all the orthogonal frequency-division multiplexing (OFDM) time parameters, resulting in a channel bandwidth of 10 MHz.

978-1-4673-2115-0/12/$31.00

The primary challenge especially for safety-related applications is to ensure a robust, latency-limited, hard-realtime, high-reliable data transmission. Beside this, the complex road environment poses a great challenge to V2X receivers. One way in order to enhance the performance V2X communication is the use of multiple antennas at the receiver side. A further possibility is tracking the channel variations during the reception of a frame, in order to increase the system performance. Applying also multiple-antennas at the transmitter, i.e. multiple-input multiple-output (MIMO) system, allows to split the transmit information into multiple streams and transfer them in parallel. MIMO systems allow both diversity and multiplexing gains. However, the current version of the IEEE 802.11p standard does not support MIMO transmission, e.g. MIMO preambles are not defined.

This paper reports on real-world measurements with receive diversity joint with pilot-assisted channel tracking in different V2V situations in a very important safety-related ITS environment, the tunnel. We focus on the low complexity scheme to update the channel transfer function from symbol to symbol tracking the time-varying channel. The authors in [5] and [6] show, based on simulations, that multiple antennas improve the performance in vehicular environments. However, the data used throughout this paper are obtained with the *V2X MIMO testbed* within the national Austrian research project ROADSAFE [7]. The testbed hardware consists of commercial off-the-shelf components, i.e. a digital signal processor (DSP) module, a field programmable gate array (FPGA) module, and a radio frequency frontend. The software running on the testbed and also for the offline processing is implemented by our own. The evaluation presented in this paper comprises the whole multi-antenna channel tracking receiver.

The remainder of the paper is organized as follows: the next section gives a brief overview of the IEEE 802.11p standard, the used measurement equipment, the different scenarios under consideration within the measurement campaign, the multi antenna receiver architecture, and the applied channel estimation and tracking schemes. The obtained results based on the frame error ratio (FER) and the frame success ratio (FSR) are presented in Section III. Finally, we summarize the contribution in Section IV.

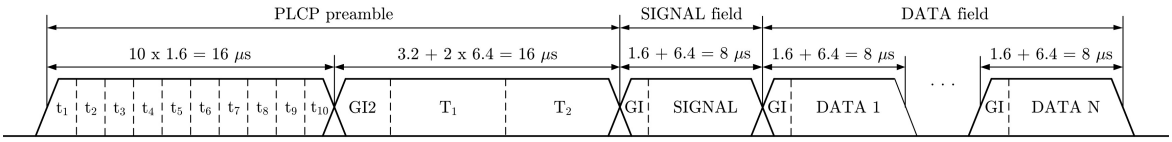

Fig. 1. IEEE 802.11p physical layer protocol data unit (PPDU) frame

II. System Description

In this section a brief summary of the PHY and the frame structure of the IEEE 802.11p standard is given. Furthermore, we present an overview of the main components of the measurement equipment, the parameter settings, the environment, and also the considered scenarios.

A. System Overview

OFDM with 64 subcarriers composes the PHY of the IEEE 802.11p standard, whereas 52 subcarriers are involved in the data transmission. Four pilot subcarriers are used to compensate the frequency and phase shifts and may also be integrated into the channel tracking process. The data are modulated, with one of the four schemes, i.e. BPSK, QPSK, 16-QAM, and 64-QAM, onto 48 data carrying subcarriers. A summary of the most important system parameters is provided in Table I.

In Fig. 1 a standard conform physical layer protocol data unit (PPDU) frame is presented. It consists of ten equal short training symbols (t_1-t_{10}) that are used for automatic gain control (AGC) and coarse time and frequency synchronization. The fine timing and frequency synchronization and also the initial channel estimation is obtained by using the two equal long training symbols (T_1,T_2). The SIGNAL field, encoded with BPSK and coding rate $1/2$, contains information about the used modulation scheme, coding rate, and length of the following data symbols. The first DATA symbol includes the 16 bit SERVICE field, whereas the first six bits are set to zero and used to initialize the descrambler at the receiver.

TABLE I
IEEE 802.11p PHY PARAMETERS

Parameter	Value
Bandwidth	10 MHz
Subcarrier spacing	156.25 kHz
FFT size	64
Used, data, pilot subcarriers	52, 48, 4
OFDM symbol duration	8 μs
Cyclic prefix duration	1.6 μs
Modualtion	BPSK, QPSK, 16-QAM, 64-QAM
Coding rate	$1/2, 2/3, 3/4$
Data rate	3, 4.5, 6, 9, 12, 18, 24, 27 Mbit/s

B. Description of the measurement campaign

The data used for the evaluation in this contribution was collected within the ROADSAFE project. The extensive V2X measurement campaign in September 2010 was located on the A4, S1, and A22 highways in the vicinity of Vienna. This paper is focused on V2V tunnel measurements located in the Kaisermühlentunnel on the highway A22.

The transmitter onboard unit (OBU), a single antenna CVIS platform [8], was placed in a Minivan. The antenna was placed in the middle of the back area on the car roof. As OBU at the receiver side the already mentioned two antenna *V2X MIMO* testbed was used. The antennas were also mounted in the back area, but at the outer corners, on the roof. All three antennas are of the same type, namely the CVIS OBU antenna [8].

The *V2X MIMO* testbed consists of standard PC equipped with a DSP module, a FPGA module from Sundance [9], and a mimoOn MORFAN radio frequency (RF) frontend [10]. In addition two external signal generators as a clock source for the down conversion into the base band and for the analog-to-digital conversion of the received signal were used. In this early stage of the testbed development only the AGC and the down sampling was implemented on the FPGA. These data were stored in a First In - First Out (FIFO) memory and transferred via the DSP to the hard disc drive of the PC. Due to limitations of the memory size and transfer rate a non continuous data stream was recorded.

The measurement was divided into three different sub-scenarios, as depicted in Fig. 2. The LOS scenario was defined such that no large trucks and only one or two cars were located between the two OBUs driving on the same lane. One big truck and several cars are located in between the transmitter and receiver in the NLOS scenario. The transmitter (OBU1) was driving in front the receiver (OBU2). In the overtaking scenario one car was overtaking the other and vice versa.

The setting was the same for all scenarios, namely a medium access control (MAC) service data unit (MSDU) packet length of 200 Bytes, a data rate of 6 Mbit/s (QPSK and coding rate

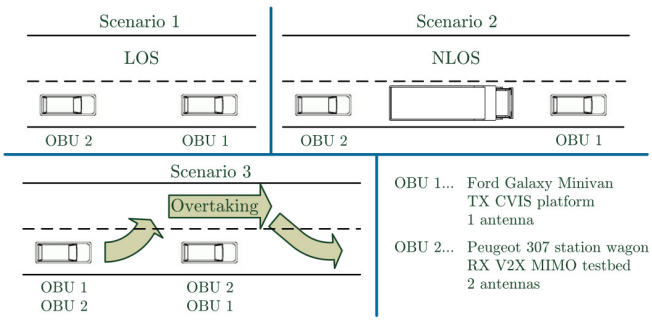

Fig. 2. Overview of the three sub-scenarios.

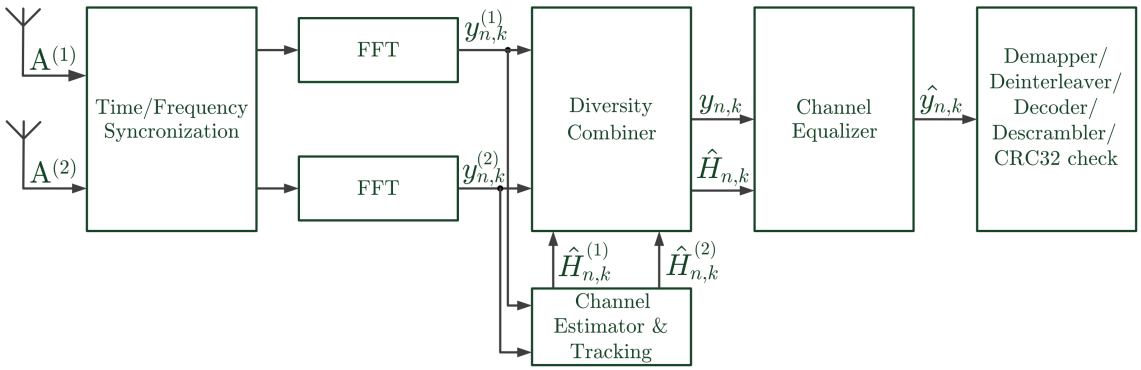

Fig. 3. IEEE 802.11p PHY block diagram.

$1/2$), a center frequency of 5880 MHz, and a broadcast (no uplink) signaling. The approximate vehicle velocity lies between 70 km/h and 100 km/h. Both test vehicles were equipped with a digital camera in the back and the front, in order to document the environment and traffic conditions during the measurement runs. More information about the testbed and the measurement campaign are found in [11].

C. Receiver Architecture

This subsection provides an overview of the implemented receiver architecture and employed algorithms. A basic block diagram is shown in Fig. 3. As already mentioned the short training symbols are used for the AGC and coarse time and frequency synchronization. The algorithm used for the synchronization process is based on the Schmidl & Cox delay-and-correlate algorithm [12]. Only the fine timing is obtained by using a cross-correlation product of the received and frequency compensated signal with a local stored version of the long preamble. In this paper we use a maximum ratio combining for the multi-antenna synchronization process, as presented in [11]. The reason is that with this technique the highest amount of frames is detected.

After removing the cyclic prefix (CP) (also called guard interval (GI)), the received time-domain signal is transferred back via a 64-point fast Fourier transform (FFT) into the frequency-domain. The IEEE 802.11p standard pilot pattern considers two kinds of pilots: the two long training symbols or *block* pilots used to obtain a channel estimate, depending on the applied estimator; afterwards only the four *comb* pilots are available for the channel estimation.

In this paper we are using three different algorithms exploiting one or both pilot pattern. The first estimator, called block averaged least squares algorithm (BALS), is based on the block pilots as follows:

$$\hat{H}^{(i)}_{n,k} = \frac{1}{2}\left(\frac{y^{(i)}_{LP1,k}}{x_{LP,k}} + \frac{y^{(i)}_{LP2,k}}{x_{LP,k}}\right), \tag{1}$$

where n represents the time index, k the subcarrier or frequency index, $^{(i)}$ the antenna stream (1 or 2), $x_{LP,k}$ the local stored long preamble, and y the first or second received long preamble symbol. This estimated channel coefficients are used for the whole frame and do not take time variations into account.

As a second estimator a comb-type least squares estimator with linear interpolation (CLS-LI) is applied. The channel transfer function is initially estimated at the pilot positions via least squares by

$$\tilde{H}^{(i)}_{n,p\mathcal{I}} = \frac{y^{(i)}_{n,p\mathcal{I}}}{x_{n,p\mathcal{I}}}, \quad \text{for} \quad 0 \le p \le P-1 \tag{2}$$

where $P = 4$ is the number of pilots, $\mathcal{I} = 14$ is the interval of the pilots, and $x_{n,p\mathcal{I}}$ is the local stored pilot subcarrier. A linear interpolator is used to obtain the remaining coefficients in-between the $p\mathcal{I}$-th and $(p+1)\mathcal{I}$-th pilot subcarrier:

$$\tilde{H}^{(i)}_{n,p\mathcal{I}+l} = \frac{\mathcal{I}-l}{\mathcal{I}}\tilde{H}^{(i)}_{n,p\mathcal{I}} + \frac{l}{\mathcal{I}}\tilde{H}^{(i)}_{n,(p+1)\mathcal{I}} \quad \begin{matrix} 1 \le l \le \mathcal{I}-1 \\ 0 \le p \le P-1 \end{matrix} \tag{3}$$

However, in the IEEE 802.11p standard not all data carrying subcarriers are in between the pilot subcarriers. Thus, edge interpolation is used for the left edge, i.e. before the first pilot subcarrier, according to

$$\tilde{H}^{(i)}_{n,p\mathcal{I}-l} = \frac{\mathcal{I}+l}{\mathcal{I}}\tilde{H}^{(i)}_{n,p\mathcal{I}} - \frac{l}{\mathcal{I}}\tilde{H}^{(i)}_{n,(p+1)\mathcal{I}}, \quad P = 0 \tag{4}$$

and similarly for the right edge, i.e. after the last pilot subcarrier,

$$\tilde{H}^{(i)}_{n,(P-1)\mathcal{I}+l} = \frac{\mathcal{I}+l}{\mathcal{I}}\tilde{H}^{(i)}_{n,(P-1)\mathcal{I}} - \frac{l}{\mathcal{I}}\tilde{H}^{(i)}_{n,(P-2)\mathcal{I}}, \quad P = 4 \tag{5}$$

where $1 \le l \le L_E$, and $L_E = 5$ are the number of the remaining subcarriers outside the pilot subcarriers. The CLS-LI algorithm is often also interpreted as a simple form of pilot-assisted channel tracking.

The third channel estimator exploits the block and comb pilots, in order to cope with channel variations. The functional principle of the pilot-assisted channel tracking with weighted average (PACT_{WA}) is as follows. At the beginning of a frame, the long preamble is used to obtain an initial channel estimate, see Eq. (1). The channel transfer function for each symbol in the frame is calculated by taking the weighted average

of the channel estimates between successive OFDM symbols according to

$$\hat{H}^{(i)}_{n,k} = (1-\gamma)\hat{H}^{(i)}_{n-1,k} + \gamma\tilde{H}^{(i)}_{n,k}\,, \tag{6}$$

where γ is the weighting factor, and $\tilde{H}^{(i)}_{n,k}$ is the channel update function, calculated via the CLS-LI algorithm, see Eqs. (2) - (5). By choosing $\gamma = 0$ the channel estimate only depends on the previous estimate, i.e. the initial channel estimate (BALS). On the other hand, select $\gamma = 1$ only the update function remains, i.e. the CLS-LI algorithm. The influence of the weighting factor will also be shown in the next section.

As combining scheme equal gain combining (EGC), with equal weighting coefficients ($\alpha = \beta = 0.5$), is used:

$$\begin{aligned} y_{n,k} = {} & \alpha\, y^{(1)}_{n,k} \exp\left(-\jmath \arg \hat{H}^{(1)}_{n,k}\right) \\ & + \beta\, y^{(2)}_{n,k} \exp\left(-\jmath \arg \hat{H}^{(2)}_{n,k}\right)\,. \end{aligned} \tag{7}$$

After the diversity combining, zero-forcing (ZF) equalization for the combined channel transfer function is performed,

$$\hat{H}_{n,k} = \alpha\,|\hat{H}^{(1)}_{n,k}| + \beta\,|\hat{H}^{(2)}_{n,k}|\,. \tag{8}$$

The simplified log-likelihood ratios (LLRs) [13] are deinterleaved and decoded with a soft-input VITERBI [14] decoder with a traceback length of 35, which corresponds to five times the constraint length of the convolutional encoder. The descrambled data is used to verify the frame check sum, a 32-bit cyclic redundancy check (CRC) number, and compare it with the received one to decide between a valid or erroneous frame.

Other blocks involved in the receiver processing are I/Q imbalance estimation and compensation, common phase error estimation and compensation, and SNR estimation that are based on algorithms documented in [15], [16], and [17].

III. Results

In this section we present the results obtained after the evaluation process with the different channel estimators for the three scenarios. As mentioned in section II-B, a data rate of 6 Mbit/s was selected, that corresponds to QPSK modulation with a coding rate of $1/2$. The payload length was set to 200 Byte which corresponds to a PPDU length of 238 Byte and a frame length of 384 μs, including preambles and SIGNAL field. We performed four LOS, two NLOS and two Overtaking measurement runs with the results averaged.

Table II shows the results in terms of the FSR for all three scenarios and the different applied channel estimation and tracking techniques. For all previous mentioned settings the two single antenna ($A^{(1)}$ and $A^{(2)}$) and multi-antenna (EGC) results are listed. The selection of the forgetting factor γ = 0.3 is explained in detail later in this section. A frame success has to pass two checks. The first is defined by a correctly received and decoded SIGNAL field. This means that the rate, length and parity bit are correct and if one of these parameters is wrong the frame is marked as incorrect. This is due to the fact that we know from the transmitter side which transmit configuration is used and therefore we are able to set them always correctly. Thus we are able to check for a correct CRC even with a wrongly decoded SIGNAL field. This behavior was only observed for eight frames in all scenarios and settings. Finally the CRC check is performed. Since not every synchronization scheme detects the same number of frames, we use the total number of possible frames in a recorded data stream, as described in [11], in order to calculate the FSR. This ensures a fair comparison throughout the whole evaluation process.

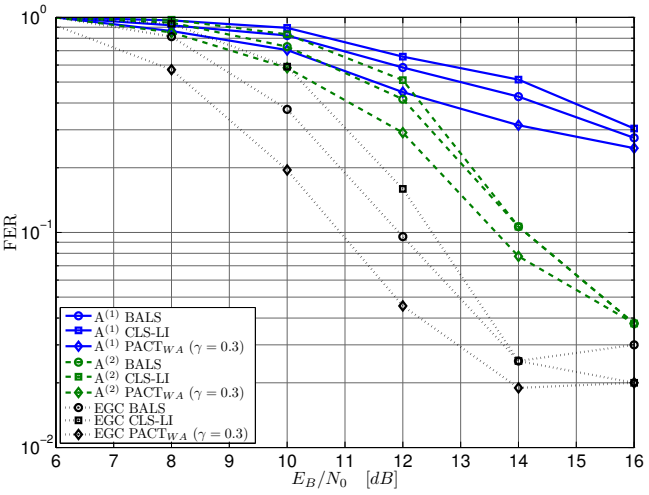

Fig. 4. FER vs. E_B/N_0 for the LOS scenario and different channel estimation techniques with and without receive diversity.

In Fig. 4 the FER against the E_b/N_0 is plotted for the LOS scenario. The solid lines correspond to the single antenna evaluation $A^{(1)}$, the dashed lines represent $A^{(2)}$, and the dotted lines the combined results. One of the first eye-catching results in Table II and Fig. 4 is the quite high performance difference between the two single antennas. The explanation for this is a difference in the RF frontend chain even if the same settings were used. This was evaluated in the laboratory, feeding the same signal to both inputs and with the result of a lower

TABLE II
Frame Success Ratio

		BALS	CLS-LI	PACT$_{WA}$ (γ=0.3)
LOS	$A^{(1)}$	18 %	14 %	25 %
	$A^{(2)}$	33 %	28 %	41 %
	EGC	59 %	48 %	71 %
NLOS	$A^{(1)}$	13 %	10 %	20 %
	$A^{(2)}$	34 %	31 %	43 %
	EGC	48 %	45 %	58 %
Overtaking	$A^{(1)}$	53 %	51 %	57 %
	$A^{(2)}$	60 %	59 %	64 %
	EGC	81 %	77 %	85 %

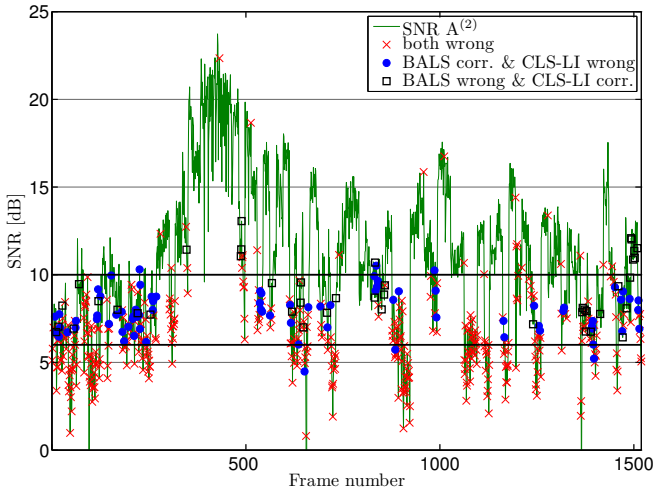

Fig. 5. Single overtaking run with block- and comb-pilot channel estimation.

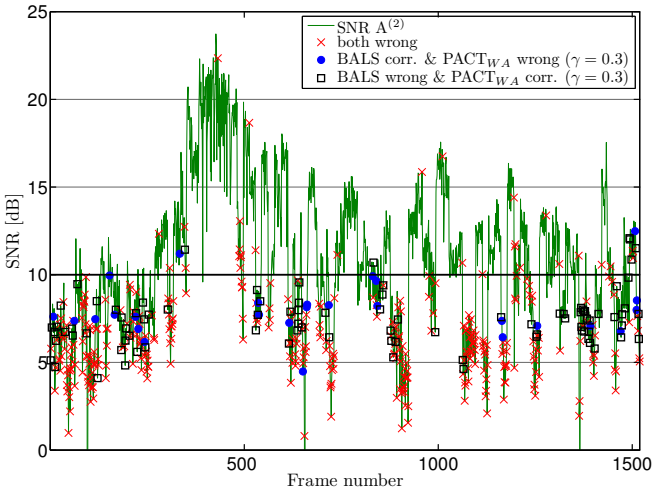

Fig. 7. Single overtaking snapshot with channel tracking.

measured power spectral density on antenna $A^{(1)}$. The AGC is able to compensate this, but the SNR at antenna $A^{(1)}$ is still lower.

Now, if we look at the results for the BALS and CLS-LI we observe differences of about 4 %-5 %, and up to 11 % in the multiantenna case, in terms of successful decoded frames. A possible explanation for this is that we were using a short packet length and also the common phase error estimation and compensation increases the performance of the BALS. Beside this explanation we observed a further behavior, see Fig. 5. Figure 5 shows the SNR of one overtaking run for a single antenna ($A^{(2)}$). The red crosses mark frames were both techniques do not receive a correct frame. The blue dots tag the case where BALS decodes correct and CLS-LI fails, with an aggregate amount of 78. The 43 black squares corresponds the other way around. It can be seen that in the SNR range between 6 dB and 10 dB the BALS is able to decode more

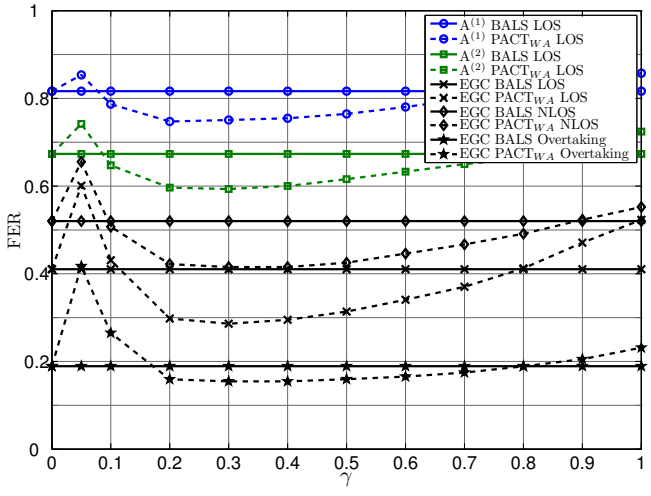

Fig. 6. Evaluation of the forgetting factor (γ) for different antenna configurations and scenarios.

frames. Whereas above the CLS-LI schemes performs a little bit better. This plot also shows the need of better channel estimation algorithms. Before we present the results obtained with the PACT_{WA} algorithm, we investigate the influence of the forgetting factor (γ) on the performance in detail.

Figure 6 shows the FER as a function of γ for the single antenna setting in the LOS scenario. Furthermore, also the behavior for the multi antenna configuration and the three scenarios is plotted. As performance indicator BALS is depicted with a solid line. Between 0.1 and 0.7 the PACT_{WA} algorithm performs always better than the BALS algorithm with a minimum FER (nearly for all scenarios) of 0.3.

This improvement is also shown in Fig. 7 where now BALS and PACT_{WA} is compared for the single overtaking snapshot. The sum of the correct and wrong decoded frames of BALS compared to PACT results in 27 and 90, respectively. Especially below 10 dB a higher amount of black squares is observable, but there are still a lot of wrong frames in these regions. However, this is also observable in Table II for all scenarios. In the NLOS scenario an improvement of up to 9 % is reached. This is because of the none (blocked) line-of-sight component most of the time, which results in a lower SNR. Therefore the tracking has a high impact. The lowest improvement (approx. 3 %) is noticed in the overtaking scenario. Here the transmitter and receiver are in line-of-sight and additional have the lowest distance between them, resulting in a higher SNR.

IV. Conclusion

We discussed performance measurements of a dual antenna IEEE 802.11p receiver with a low-complexity pilot-assisted channel tracking scheme. The evaluation is based on real-world measurement data in a vehicular tunnel environment including line-of-sight, non line-of-sight, and overtaking scenario, with an approximate vehicle velocity between 70 km/h and 100 km/h.

We show that even with simple techniques (equal gain combining and pilot-assisted channel tracking with weighted average) the frame success ratio is improved significantly. The increased performance in terms of the frame success ratio is up to 38 % in the line-of-sight scenario using two antennas and the low-complexity pilot-assisted channel tracking scheme. Even in the non line-of-sight scenario up to 24 % more frames are successfully decoded. We further show that the optimum forgetting factor, in the case pilot-assisted channel tracking with weighted average, is 0.3 - independent of the selected antenna configuration and/or the chosen scenario. A diversity gain of up to 1.5 dB is achieved at a frame error ratio of 10 %, compared to a standard comb pilot based channel estimation algorithms. We expect that driving with higher speed and/or increasing the frame length will further increase the FER.

ACKNOWLEDGMENT

This work has been funded by the Christian Doppler Laboratory for Wireless Technologies for Sustainable Mobility. The financial support by the Federal Ministry of Economy, Family and Youth and the National Foundation for Research, Technology and Development is gratefully acknowledged. We acknowledge the Federal Ministry for Transport, Innovation, and Technology of Austria (BMVIT) for granting a test license in the 5.9 GHz band. We would specially like to thank our industrial partner Kapsch TraffiCom AG for enabling this work and supporting us with many advices and discussions.

REFERENCES

[1] "Special issue on vehicular communications," *Proceedings of the IEEE*, vol. 99, no. 7, Jul. 2011.

[2] *European profile standard for the physical and medium access control layer of intelligent transport systems operating in the 5 GHz frequency band*, ETSI Std. final draft ETSI ES 202 663 V1.1.0, Nov. 2009.

[3] *IEEE Standard for information technology-Telecommunications and information exchange between systems-Local and metropolitan area networks-Specific requirements Part 11: Wireless LAN Medium Access Control (MAC) and Physical Layer (PHY) Specifications - Amendment 6: Wireless Access in Vehicular Environments*, IEEE Standard 802.11p-2010, Jul. 2010.

[4] *IEEE 802.11a, Part 11: Wireless LAN Medium Access Control MAC and Physical Layer PHY Specifications High-speed Physical Layer in the 5 GHz Band*, ETSI Std. 802.11a-1999(R2003), Jun. 2003.

[5] A. Bourdoux, H. Cappelle, and A. Dejonghe, "Channel tracking for fast time-varying channels in IEEE802.11p systems," in *Proc. IEEE Global Telecommunications Conference, (GLOBECOM 2011)*, Houston, Texas, USA, Dec. 2011, p. 6.

[6] J. Nuckelt, H. Hoffmann, M. Schack, and T. Kürner, "Linear diversity combining techniques employed in Car-to-X communication systems," in *Proc. 73rd IEEE Vehicular Technology Conference, (VTC2011-Spring)*, Budapest, Hungary, May 2011, pp. 1–5.

[7] ROADSAFE. [Online]. Available: http://www.ftw.at/projects/roadsafe

[8] CVIS. [Online]. Available: http://www.cvisproject.org/

[9] Sundance Multiprocessor Technology. [Online]. Available: http://www.sundance.com/

[10] mimoOn. [Online]. Available: http://www.mimoon.de/

[11] G. Maier, A. Paier, and C. F. Mecklenbräuker, "Packet detection and frequency synchronization with antenna diversity for IEEE 802.11p based on real-world measurements," in *Proc. International ITG Workshop on Smart Antennas, WSA 2011*, Aachen, Germany, Feb. 2011, pp. 1–7.

[12] T. M. Schmidl and D. C. Cox, "Robust frequency and timing synchronization for OFDM," *IEEE Transactions on Communications*, vol. 45, no. 12, pp. 1613–1621, Dec. 1997.

[13] F. Tosato and P. Bisaglia, "Simplified soft-output demapper for binary interleaved COFDM with application to HIPERLAN/2," in *Proc. IEEE International Conference on Communications, ICC 2002*, vol. 2, New York, NY, USA, Apr./May 2002, pp. 664–668.

[14] A. J. Viterbi, "Error bounds for convolutional codes and a asymptotically optimum decoding algorithm," *IEEE Transactions on Information Theory*, vol. IT-13, no. 2, pp. 260–269, Apr. 1967.

[15] I. Held, O. Klein, A. Chen, and V. Ma, "Low complexity digital IQ imbalance correction in OFDM WLAN receivers," in *Proc. IEEE 59th Vehicular Technology Conference, VTC 2004-Spring*, vol. 2, Milan, Italy, May 2004, pp. 1172–1176.

[16] G. Maier, A. Paier, and C. F. Mecklenbräuker, "Performance evaluation of IEEE 802.11p infrastructure-to-vehicle real-world measurements with receive diversity," in *Proc. 8th International Wireless Communications and Mobile Computing Conference, IWCMC-2012*, Limassol, Cyprus, Aug. 2012, p. 6.

[17] G. Ren, H. Zhang, and Y. Chang, "SNR estimation algorithm based on the preamble for OFDM systems in frequency selective channels," *IEEE Transactions on Communications*, vol. 57, no. 8, pp. 2230–2234, Aug. 2009.